ELSEVIER

Journal of Magnetism and Magnetic Materials 225 (2001) 138–144

Journal of magnetism and magnetic materials

www.elsevier.com/locate/jmmm

A DNA array sensor utilizing magnetic microbeads and magnetoelectronic detection

M.M. Miller*, P.E. Sheehan, R.L. Edelstein, C.R. Tamanaha, L. Zhong, S. Bounnak, L.J. Whitman, R.J. Colton

Naval Research Laboratory, Washington, DC 20375, USA

Abstract

We describe a multi-analyte biosensor that uses magnetic microbeads as labels to detect DNA hybridization on a micro-fabricated chip. The beads are detected by giant magnetoresistance (GMR) magnetoelectronic sensors embedded in the chip. The prototype device is a tabletop unit containing electronics, a chip carrier with a microfluidic flow cell, and a compact electromagnet and is capable of simultaneous detection of eight different analytes. © 2001 Published by Elsevier Science B.V.

Keywords: Biosensor; GMR; Magnetoelectronics; DNA array; DNA hybridization; Magnetic beads

Over the past several years research in magnetic label-based bioassays has become an area of increasing interest. However, most of these schemes have used bulk detection techniques such as AC susceptometry or SQUID magnetometry [1,2]. Such techniques are relatively simple and, by using SQUID-based sensors, may allow ultra high sensitivity. However, because SQUID-based sensors require expensive cryogenics and instrumentation, adapting these techniques to a practical, multi-analytical sensor is not readily foreseeable. Recently, a biosensor using micron-sized magnetic bead (microbead) labeling and giant magnetoresistance (GMR) sensor arrays was proposed [3]. This sensor is referred to as BARC (for Bead Array Counter), and many aspects of the system have been described previously [3,4].

The core of the BARC device is a chip containing microfabricated GMR magnetic field sensors. First reported in 1988 [5], GMR materials are thin films of alternating magnetic and non-magnetic layers. The resistance of these films depends on the relative orientation of the magnetic moments of the layers. These magnetic moments can be varied by an applied magnetic field that in turn varies the resistance. Because of their many favorable properties, these materials have been utilized in many applications such as magnetic field sensors and hard drive read heads. In the next few years, GMR-based non-volatile random access memory is expected to be commercialized [6]. While GMR-based magnetoresistive sensors are not as intrinsically sensitive as SQUIDS, in practice when used to measure the magnetic field generated by a micron-scale magnetic particle these devices can be more sensitive (owing to the extreme proximity of the particle to the sensor). In this paper, we report preliminary

* Corresponding author.
E-mail address: michael.miller@nrl.navy.mil (M.M. Miller).

0304-8853/01/$ - see front matter © 2001 Published by Elsevier Science B.V.
PII: S0304-8853(00)01242-7

Report Documentation Page

Form Approved
OMB No. 0704-0188

Public reporting burden for the collection of information is estimated to average 1 hour per response, including the time for reviewing instructions, searching existing data sources, gathering and maintaining the data needed, and completing and reviewing the collection of information. Send comments regarding this burden estimate or any other aspect of this collection of information, including suggestions for reducing this burden, to Washington Headquarters Services, Directorate for Information Operations and Reports, 1215 Jefferson Davis Highway, Suite 1204, Arlington VA 22202-4302. Respondents should be aware that notwithstanding any other provision of law, no person shall be subject to a penalty for failing to comply with a collection of information if it does not display a currently valid OMB control number.

1. REPORT DATE	2. REPORT TYPE	3. DATES COVERED
2001		**00-00-2001 to 00-00-2001**

4. TITLE AND SUBTITLE	5a. CONTRACT NUMBER
A DNA array sensor utilizing magnetic microbeads and magnetoelectronic detection	5b. GRANT NUMBER
	5c. PROGRAM ELEMENT NUMBER
6. AUTHOR(S)	5d. PROJECT NUMBER
	5e. TASK NUMBER
	5f. WORK UNIT NUMBER
7. PERFORMING ORGANIZATION NAME(S) AND ADDRESS(ES) **Naval Research Laboratory,4555 Overlook Avenue SW,Washington,DC,20375**	8. PERFORMING ORGANIZATION REPORT NUMBER
9. SPONSORING/MONITORING AGENCY NAME(S) AND ADDRESS(ES)	10. SPONSOR/MONITOR'S ACRONYM(S)
	11. SPONSOR/MONITOR'S REPORT NUMBER(S)

12. DISTRIBUTION/AVAILABILITY STATEMENT
Approved for public release; distribution unlimited

13. SUPPLEMENTARY NOTES

14. ABSTRACT
We describe a multi-analyte biosensor that uses magnetic microbeads as labels to detect DNA hybridization on a micro-fabricated chip. The beads are detected by giant magnetoresistance (GMR) magnetoelectronic sensors embedded in the chip. The prototype device is a tabletop unit containing electronics, a chip carrier with a microfluidic flow cell, and a compact electromagnet and is capable of simultaneous detection of eight di!erent analytes.

15. SUBJECT TERMS

16. SECURITY CLASSIFICATION OF:			17. LIMITATION OF ABSTRACT	18. NUMBER OF PAGES	19a. NAME OF RESPONSIBLE PERSON
a. REPORT	b. ABSTRACT	c. THIS PAGE			
unclassified	**unclassified**	**unclassified**	**Same as Report (SAR)**	**7**	

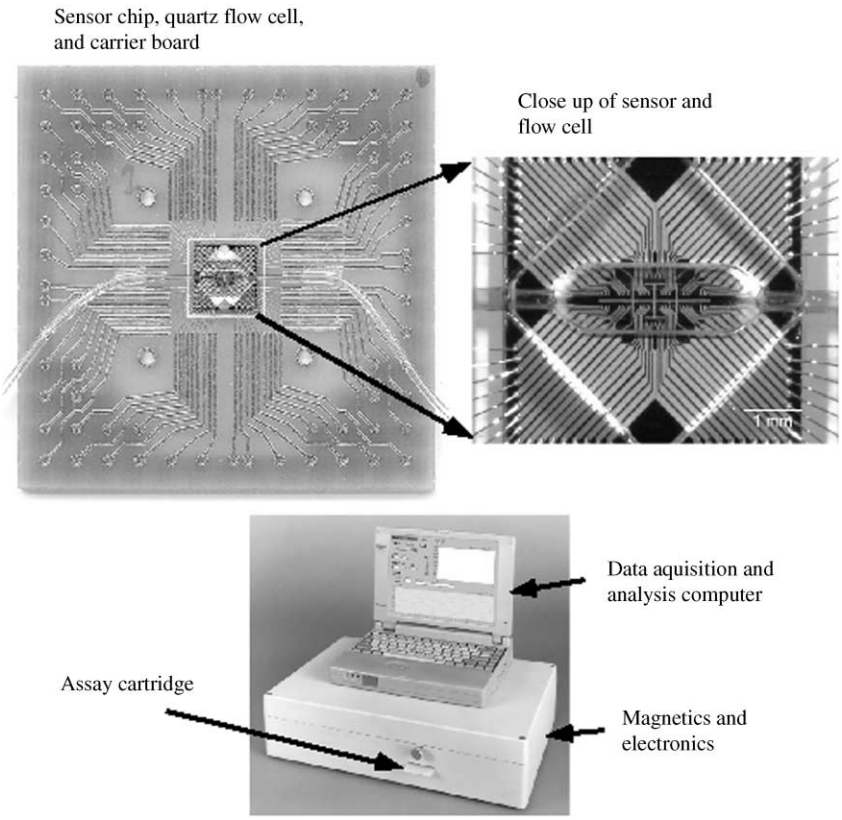

Fig. 1. Different aspects of the BARC sensor prototype. The lower image is the table top unit containing all electronics, electromagnet, assay cartridge (with BARC chip, flow cell, etc.), and computer. The upper left image is the BARC chip with flow cell mounted on the chip carrier board which is mounted in the assay cartridge. The upper right image is a magnified view of the 5 mm × 5 mm BARC chip with flow cell.

measurements in which we have detected DNA hybridization on the BARC chip, and discuss important magnetic issues related to further development of the BARC sensor.

The BARC prototype we are developing is a tabletop instrument consisting of a microfabricated chip (solid substrate) with an array of GMR sensors, a chip carrier board with electronics for lock-in detection, a fluidics cell and cartridge, and an electromagnet. Some of these elements are shown in Fig. 1. We currently use a GMR sensor chip fabricated by Nonvolatile Electronics, Inc. (NVE, Eden Prairie, MN) in which the GMR sensor geometry (80 μm × 5 μm sensor strips) has been optimized for detection [3]. These strips are connected to 1 μm-thick aluminum leads (traces) designed to minimize resistance, which terminate in wirebond pads in the corners of each chip. To facilitate connection with the electronics, the BARC chip is wirebonded to a chip carrier board. The chips are 5 mm × 5 mm and were designed to allow integration with fluidics. Finally, the surface of the chip is sputter-coated with a 1 μm-thick silicon nitride layer to passivate the surface against the electrolytic solution that is present during an assay.

The proprietary GMR sensors essentially consist of two magnetic layers separated by a thin copper spacer and have a total thickness of approximately 10 nm. These sensors are generally used in magnetic field sensing applications, detecting the component of a uniform magnetic field parallel to the uniaxial sensitivity axis. However, the magnetic field from a microbead, which is much smaller than the sensor, is highly localized (as will be discussed below).

Nevertheless, the detection of single microbeads with these sensors has been demonstrated [3,4].

The BARC chip contains clusters of sensors in order to increase the sensitivity of the assay. Optimal signal to noise is expected when a GMR sensor is covered by a single bead [7]. However, the chemical sensitivity, or number of analyte molecules that can hybridize to the surface, increases with increasing surface area. Therefore, a cluster of small sensors allows for both chemical and instrumental sensitivity. The ideal sensor array would contain many thousands of 'single bead' sensor elements and would be akin to GMR-based random access memory chips currently under development [3,4,7]. For a variety of reasons, such an array is technically difficult to fabricate and the present prototype represents a more realistic approach at the present time.

To understand better how microbeads are detected by the GMR sensor, we consider the magnetization of a sphere. It is well-known that a uniformly magnetized sphere can be described purely as a dipole (no higher multipoles) at the center of the sphere with a magnetic field, $\boldsymbol{B}$, at some distance r given by [8]

$$\boldsymbol{B}(\boldsymbol{r}) = \frac{3\hat{r}(\hat{r}\cdot\boldsymbol{m}) - \boldsymbol{m}}{r^3}, \tag{1}$$

where $\boldsymbol{m}$ is the magnetic moment of the sphere. The BARC GMR elements are sensitive to magnetic fields in the sensor plane and particularly along a uniaxial direction (x-axis) that is parallel to the long axis of the sensor. We will consider a coordinate system in which the plane of the GMR sensor is coincident with the x–y plane while the external magnetic field that magnetizes the bead with a moment $\boldsymbol{m} = m\hat{z}$ is along z (see Fig. 2). Provided this magnetizing field H_z is well below fields necessary to magnetize the layers of the GMR sensor along z ($\sim 10^4$ Oe), only the planar components of the microbead field will induce an appreciable magnetoresistance. Furthermore, the planar component of the field from the bead is axially symmetric, so it is natural to change to cylindrical coordinates in which this purely radial component is given by

$$B_\rho = \frac{3mz\rho}{r^5} \tag{2}$$

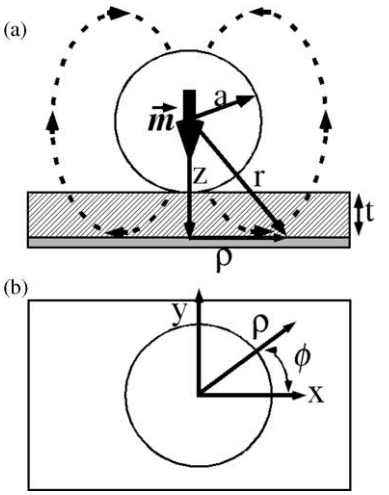

Fig. 2. Coordinate system for a microbead relative to a sensor plane. (a) Side view, (b) top view.

with

$$r = \sqrt{z^2 + \rho^2}. \tag{3}$$

The distance from the bead center to the sensor plane is given by

$$z = a + t \tag{4}$$

where a is the bead radius and t is the separation of the bottom of the bead and the GMR sensor (Fig. 2). (In the case of the BARC sensor, t is the thickness of the silicon nitride passivation layer combined with that of relatively thin gold layer plus the thickness of chemical species that are used to immobilize the bead at the surface.) B_ρ is strongly dependent upon ρ and z and reaches a maximum value

$$B_\rho^{\max} = B_\rho(z/2) = \frac{3}{2}\left(\frac{4}{5}\right)^{5/2}\frac{m}{z^3} = 0.86\frac{m}{z^3}. \tag{5}$$

The radial dependence of this field is shown in Fig. 3 for different separations, where $z = 1.7a$ (1.7 times the bead radius) corresponds to the present BARC sensor (with a 1 μm-thick passivation layer and 2.8 μm-diameter bead presently used). This field profile peaks sharply, with the peak moving radially outward as z increases. Furthermore,

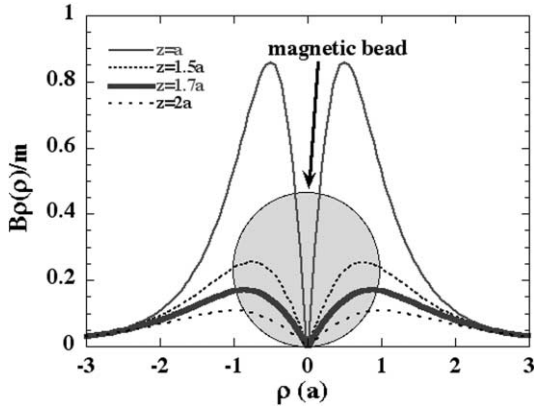

Fig. 3. The radial planar component of a magnetic field, normalized by the moment m, for different bead surface separations z given in units of bead radius a. For $z = a$, the bead is on the surface.

the BARC sensors are only sensitive to the x-component of the magnetic field, given by

$$B_x = B_\rho \cos\phi, \tag{6}$$

where ϕ is the angle between the radial direction and x as shown in Fig. 2. Therefore, the magnetic field detected by the sensor is limited to two lobes closely confined to the bead as shown in Fig. 3 (see also Ref. [3]). A bead typically affects a sensor area roughly equal to that physically covered by the bead and the resistance of the sensor is roughly proportional to the number of magnetic beads on the sensor at low bead coverage.

To detect the magnetic beads on top of a GMR strip, a magnetic field is applied along the z-axis using a custom designed electromagnet integrated with the BARC chip and fluidics cartridge. This electromagnet produces fields that are parallel to the z-axis. The BARC chip has 64 identical sensor elements (arranged in groups of eight) plus two reference elements identical to the sensor elements. Sensor-reference pairs are selectable to form half of a Wheatstone bridge. The other half of the bridge is contained in the electronics module off the chip. The signal from each sensor bridge is measured by applying an AC magnetizing-field (~ 100 Oe rms at 200 Hz) with the electromagnet, and detecting the bridge signals with a lock-in amplifier [4]. Each signal is measured 64 times and the results averaged.

Analytes and microbeads are introduced through a microfluidics system that is being developed to ensure uniform sample and bead flow over the sensor, maximize sensor sensitivity, and minimize assay time. Presently, this consists of a quartz flow cell into which the fluids are introduced through tubing using an external peristaltic pump. Eventually, an integrated fluidics cartridge complete with reservoirs and miniature displacement pumps and valves will be incorporated [4].

Although BARC could, in principle, be used to detect a wide variety of molecular recognition reactions, we are initially using DNA hybridization to detect various biological warfare agents. DNA probes are arrayed on the sensor chip using the following procedure: A thin (~ 80 nm) layer of gold is thermally evaporated over the sensor areas using lift-off lithography. Additionally, 1 μm-thick hexagonal 'mesas' are patterned over the reference sensors to reduce any undesired signal to these elements should stray microbeads become nonspecifically bound over those sensors. Immediately prior to DNA patterning, the gold surfaces are cleaned by a 'descumming' process that consists of a 15 min exposure in a 250 mTorr oxygen plasma in order to remove any residual organics. Single-stranded DNA oligomers (approximately 30 nucleotides long) which are thiolated at the 3′-end are spotted onto the gold surface directly above the GMR sensors using micro-contact pen spotting [4]. The quartz flow cell is then attached using UV-curing epoxy.

The analyte DNA samples are biotin labeled. When a particular analyte is injected into the instrument, it hybridizes with the probe(s) on the chip having the complementary sequence. Streptavidin-labeled magnetic beads are then added and specifically bind to the biotinylated sample DNA on the chip surface. Although it was initially planned to employ a magnetic field gradient to remove any beads bound by weak, nonspecific interactions, enabling force discrimination as part of the assay [3], we have found that these beads can be simply and effectively removed by rinsing with a buffer solution. The GMR sensors detect the beads remaining on the surface, and the intensity and location of the

signal indicate the concentration and identity of pathogens present in the sample.

Assays presently utilize M-280 'Dynabeads' (Dynal, Inc., Lake Success, NY) as labels. These microbeads are 2.8 μm-diameter polystyrene spheres impregnated with ~ 15 nm diameter γ-Fe_2O_3 particles that compose about 6% of the total volume of the bead. These particular beads were chosen because they are non-remnant (and therefore are less likely to agglomerate), they are pre-labeled with streptavidin, and previous studies have shown that they can be detected by the BARC GMR sensors.

To demonstrate the selectivity of the hybridization and magnetoelectronic detection we patterned four different probes over pairs of eight-sensor arrays on a BARC chip. Three probes consisted of single stranded DNA oligomers from *Botulinum* neurotoxin B (BB), *Francisella tularensis* (FT), and *Yersinia pestis* (YP). Additionally, a positive control (PC) consisting of a biotinylated single strand DNA-oligomer was also attached in order to test the streptavidin-biotin recognition and binding, i.e., the magnetic beads should always bind at this site. In a particular assay, a sample of FT was introduced as the analyte. Fig. 4a shows an image of the sensor area after hybridization and bead immobilization. The various probes areas are indicated in the figure. Fig. 4b shows a plot of the response for the individual 64 sensors (16/probe) as well as the sum of these 16 signals for each probe. Clearly, the FT sample registered on the correct probe with a signal level 10 times higher than the 'background' of BB and YP and about 75% the signal from the positive control.

While we have shown the BARC device will reliably detect a specific DNA hybridization event, further refinements are underway. The magnetic field at the sensor from a microbead decreases rapidly with bead-sensor separation as z^{-3}. In a forthcoming chip design that will have 64 sensor areas, we will reduce the silicon nitride layer thickness directly over the sensors from 1 μm to less than 0.5 μm, which should more than double the GMR response to an M-280 microbead. It is conceivable that the passivation layer can be thinned to below 0.1 μm thick, resulting in a greater than four-fold increase in sensitivity.

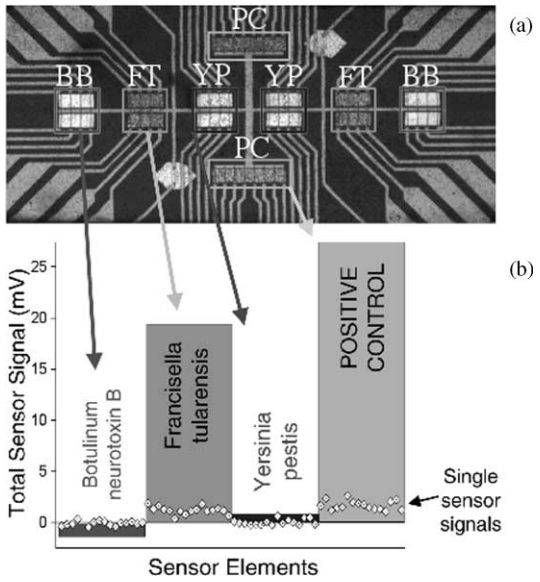

Fig. 4. (a) Image of BARC sensor chip with the flow cell (after bead immobilization) detailing the location of the various DNA probes. The bright rectangular areas (darkened where bead density is high) are the patterned gold surfaces. The hexagonal 1 μm thick gold mesas covering the reference elements are also visible. (b) The signal output of the BARC sensor chip from an FT assay. The individual sensor signals sensor (8/probe site, 16/probe) are plotted along with the sum of these signal for each probe.

Still greater improvement can be realized by employing microbeads with higher 'magnetic density'. Because the M-280 beads contain a very low volume fraction of magnetic material, the resulting magnetization is greatly reduced compared to that of a bead that is 100% magnetic. To maximize the potential signal from a magnetic label, the microbead should consist of a soft ferromagnetic material, e.g., iron or a NiFe alloy. (We assume that issues such as surface passivation and functionalization of the microbead with biomolecules can be feasibly addressed, perhaps via gold encapsulation.) Soft ferromagnetic beads can provide enhanced performance because they provide the maximum obtainable susceptibility, and they will have a greater saturation magnetization M_s, resulting in the largest inducible moments for a given bead size. Finally, because these soft ferromagnets would be spherical and have very low coercivity, the shearing of the $M(H)$ loop due to demagnetization will effectively eliminate remnance.

The above arguments follow from considering the magnetization of a highly permeable sphere in a uniform magnetic field given by [8,9]

$$\boldsymbol{M} \approx \frac{3}{4\pi}\boldsymbol{H}. \tag{7}$$

While Eq. (7) is generally given for paramagnetic spheres, in the case of soft ferromagnetic material — where the coercive field H_c is much less than the demagnetizing fields — this result will hold. However, as the bead diameter approaches the single domain size limit Eq. (7) will no longer hold. We estimate that a microbead with a diameter larger than 0.1–0.2 μm will suffice based on calculations for zero anisotropy spheres [10]. Any highly permeable sphere will have the same magnetization for applied fields below the saturation field,

$$H_s = \frac{4\pi}{3}M_s, \tag{8}$$

where the saturation magnetization M_s will depend upon the material [9]. Fig. 5 shows the magnetization curves given by Eq. (7) (dashed lines) with the horizontal lines representing M_s for various materials. The shaded areas represent the ranges of M_s for some typical ferrimagnetic and ferromagnetic materials. Specifically, the upper bound of the ferromagnets is for Fe and the lower bound is NiFe. The solid curves represent the magnetizations measured for samples of $Ni_{70}Fe_{30}$ (NiFe) powder and M-280 microbeads. The NiFe powder (Novamet, Wyckoff, NJ) ranges in diameter from approximately 1 to 10 μm with an average diameter of about 3 μm. Presumably, the magnetization curve deviates from the ideal due to non-spherical particles and clusters of particles in this bulk sample measurement. Again, we note that the M-280 magnetization is well below that expected for a solid ferrimagnetic sphere of the same material. Using $\boldsymbol{m} = \boldsymbol{M}V$ (V is the bead volume) we can use Eq. (5) to make the following estimates for $H = 100$ Oe: From the magnetization curves we expect $B_\rho^{\max} \approx 3.2$ and 29 Oe for M-280 and NiFe beads, respectively, while, theoretically, we expect these values should be approximately 1 and 17 Oe. We have compared the response of a BARC sensor element to NiFe beads and M-280 beads of the same size. Under identical conditions, with an applied magnetizing field $H_z = 100$ Oe, the NiFe microbead yields 12 times the signal of the M-280 microbead — a value midway between the expected signal. Furthermore, without an external magnetic field, the sensor does not detect the NiFe particles, indicating low remanance. These considerations (using a 1 μm-thick passivation layer) also reveal that a 0.8 μm-diameter NiFe bead produces the same maximum field as the much larger M-280. Also shown in Fig. 5 are the expected magnetization ranges for ferrimagnetic beads. Note that in situations that allow for the application of magnetic fields in excess of 2 kOe, ferromagnetic beads will exceed the magnetization of *any* ferrimagnetic bead.

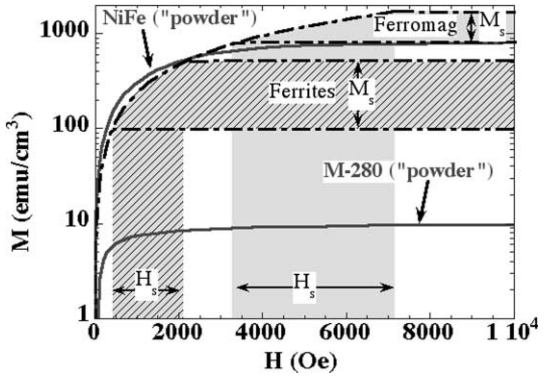

Fig. 5. (a) Solid curves: Magnetization curves for NiFe and M-280 'powder' samples. Dashed curves: theoretical magnetization curves for a sphere. The horizontal lines are saturation values for various materials; the shaded areas indicate ranges for ferrimagnets and ferromagnets.

In conclusion, we have shown that a multi-analyte biosensor utilizing GMR sensor arrays can selectively detect specific DNA-hybridization in the presence of multiple probes. We are presently developing a 64-analyte BARC chip that will require refinements to the chip design. Finally, by using ferromagnetic microbeads it may be possible to fabricate BARC chips capable of simultaneous assays of thousands of analytes.

This work was supported by the Defense Advanced Research Projects Agency. CRT is an American Society for Engineering Education

post-doctoral fellow and PES is a National Research Council Postdoctoral Research Associate. We would like to thank Drs. G. Prinz, P. Lubitz, K. Bussmann, J. Byers, E. Carpenter and D. Baselt for useful discussions. We would also like to thank K. Lee for technical assistance on the electronics, and G. Long and C. Drombetta from NMRC for the DNA probe sequences.

References

[1] C.B. Kriz, K. Radevik, D. Kriz, Anal. Chem. 68 (1996) 1966.
[2] R. Kötitz, H. Matz, L. Trahms et al., IEEE Trans. Appl. Supercond. 7 (1997) 3678.
[3] D.R. Baselt, G.U. Lee, M. Natesan et al., Biosens. Bioelectron. 13 (1998) 731.
[4] R.L. Edelstein, C.R. Tamanaha, P.E. Sheehan et al., Biosens. Bioelectron. 14 (1999) 805.
[5] M.N. Baibich, J.M. Broto, A. Fert et al., Phys. Rev. Lett. 61 (1988) 2472.
[6] G.A. Prinz, Science 282 (1998) 1660.
[7] M. Tondra, M. Porter, R. Lipert, J. Vac. Sci. Technol. 18 (2000) 1125.
[8] J.D. Jackson, Classical Electrodynamics, 2nd edition, Wiley, New York, 1975, p. 195.
[9] S. Chikazumi, Physics of Magnetism, Wiley, New York, 1964, p. 23.
[10] A. Aharoni, J. Appl. Phys. 5 (1981) 993.